Journal of Material Science and Mechanical Engineering (JMSME)
Print ISSN: 2393-9095; Online ISSN: 2393-9109; Volume 2, Number 2; January-March, 2015 pp. 134-139

http://www.krishisanskriti.org/jmsme.html

Combined Energy, Exergy and Optical Analyses of Flat Plate Solar Thermal Collector using Nanofluids

Satish Upadhyay[1], Jahar Sarkar[2] and Rashmi Rekha Sahoo[3]

[1]Mechanical Engineering Deptt Indian Institute of Technology (B.H.U.) Varanasi, UP-221005
[2]Mechanical Engineering Deptt Indian Institute of Technology (B.H.U.) Varanasi, UP-221005
[3]Mechanical Engineering Deptt Indian Institute of Technology (B.H.U.) Varanasi, UP-221005
E-mail: [1]satish.mec12@itbhu.ac.in, [2]js_iitkgp@yahoo.co.in, [3]rrs_iitbhu@rediffmail.com

Abstract—*In this paper, the energy analysis, exergetic analysis and optical analysis have been performed to determine design parameters and optical performance of solar flat plate collector using nanofluids. Absorber plate area has been optimized as well. Results have been also compared with conventional fluids. Present results show that using nanofluids instead of conventional fluids improves the heat transfer as well as optical and thermal properties, and efficiencies (1st and 2nd law efficiency) of flat plate solar thermal collector. Effects of various operating and design parameters like mass flow rate, ambient temperature, wind speed, optical efficiency, collector geometry, inlet fluid temperature on heat removal factor, collector efficiency, irreversibility and second law efficiency are discussed. For studied operating conditions, optimum values of absorber plate area mass flow rate collector efficiency have been calculated as 9.18 m^2, 0.0087kg/s and 46.8%, respectively. Finally exergetic optimization has been carried out under given design and operating conditions.*

1. INTRODUCTION

Since the emergence of nanofluids, which show higher thermal conductivities and improved thermophysical properties than the corresponding base fluids research work has investigated the potential of nanofluids as the working fluids of solar thermal collectors, whereas and this research can be classified mainly into two categories: direct absorption solar radiation that requires design changes and regular collectors that employ nanofluids as the working fluids [1-5]. Within last decade, huge amount of both numerical and experimental researches on various solar thermal coolectors using nanofluids of various nanoparticles (alumina, titanium oxide, carbon nanotubes, graphite, silver, etc.) indicated that the addition of nanoparticles to the conventional working fluids (water, ethylene glycol and heat transfer oils etc.) can improve efficiency of a flat-plate type solar collector [6-11]. Use of nanofluids in solar collector not only improves the heat transfer coefficient, also the presence of these nanoparticles enhances the absorption characteristics. Some studies were made on the potential of size reduction of various solar collectors by using nanofluids. Smaller size solar collector can reduce the material usage, cost, emission and energy required in manufacturing. Sarkar [12] proposed supercritical carbon dioxide as collector fluid and showed that carbon dioxide may better than nanofluid, however, that can be used for low temperature only. Hence, it is clear that nanofluid is a promising substitute of the conventional fluids in solar thermal collector. However, rigorous numerical as well experimental studies are still needed for practical implementation

In this paper, a procedure to simulation and optimization of flat plate solar collectors based on exergy analysis is developed. The exergy analysis of the solar collector is parametrically dependent on its optical and energy analysis. Hence firstly the optical and energy analysis of the flat plate solar collector will be carried out. Then, the solar collector exergy efficiency will be computed and optimized.

2. MATHEMATICAL MODELING

All printed material, including text, illustrations, and charts, must be kept within a print area of 6-7/8 inches (17.5 cm) wide by 8-7/8 inches (22.54 cm) high. Do not write or print anything outside the print area. All text must be in a two-column format. Columns are to be 3-1/4 inches (8.25 cm) wide, with a 5/16 inch (0.8 cm) space between them.

The following assumptions have been made for the analysis of solar collector (Fig. 1):

1. Steady state conditions.
2. Inlet temperature equals to ambient temperature.
3. Thermophysical properties of the working fluid is assumed to be constant.
4. Overall heat transfer of the heat loss is assumed to be constant.
5. Collector tilt is assumed to be constant($\beta=20^0$).
6. Nanofluids acts as a single phase and are well prepared with an adequate stability

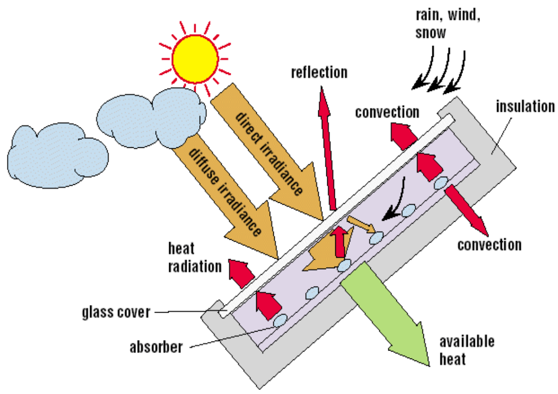

Fig. 1: Layout of flat plate collector

2.1 Energy analysis

The proof of governing equations on the solar collector energy analysis is not included to have a brief note. The useful heat gain (Q_u) by the working fluid is

$$Q_u = \dot{m}C_p(T_{out} - T_{in}) \quad (1)$$

where T_{in}, T_{out}, C_p and m are the fluid inlet, outlet temperature, heat capacity and mass flow rate of the agent fluid, respectively. The Hottel–Whillier equation for the useful heat gain (Q_u) of a flat plate solar collector system, considering the heat losses from the solar collector to the atmosphere, is

$$Q_u = A_p\, F_R\, (S - U_l(T_{in} - T_a)) \quad (2)$$

where T_a is the ambient temperature and the heat removal factor F_R is defined as

$$F_R = \frac{\dot{m}C_p}{U_l A_p}\left(1 - \exp\left(-\frac{F' U_l A_p}{\dot{m}C_p}\right)\right) \quad (3)$$

where F' is the collector efficiency factor. An energy balance on the absorber plate yields the following equation for a steady state [13].

$$Q_u = A_P S - U_l A_P (T_p - T_a) \quad (4)$$

In Eqs. (2)–(4), T_p, S and A_p are the average temperature of the absorber plate, radiation absorbed flux by unit area of the absorber plate and area of the absorber plate, respectively. Overall loss coefficient (U_L),which during the previous studies assumed as a constant factor or a variable with little effect; whereas it is not constant. The calculation of the overall loss coefficient (U_L) is based on simulation convection and re-radiation losses from the absorber plate to the atmosphere that the proof of them is not included here to have a brief note. Thermal efficiency of the solar collector is given by [13].

$$\eta_{en} = \frac{Q_u}{I_T A_p} \quad (5)$$

where I_T is the incident solar energy per unit area of the absorber plate.

2.2 Optical analysis

The energy absorbed after the optical loss is calculated by

$$S = I_b R_b(\tau\alpha)_b + I_d\ (\tau\alpha)_d(1+\cos\beta/2) + \rho_g I\ (\tau\alpha)_g(1-\cos\beta/2)$$

In Eq. (2) the radiation absorbed flux by unit area of the absorber plate (S) is defined as

$$S = (\tau\alpha)_{av} I_T \quad (6)$$

where $(\tau\alpha)_{av}$ is the effective product transmittance–absorptance that is equal with the optical efficiency (η_o) [13].

2.3 Exergy analysis

Exergy is defined as maximum amount of work which can be produced by a system or energy as it comes to equilibrium with a reference environment.

$\dot{E}_{in} + \dot{E}_S + \dot{E}_{out} + \dot{E}_l + \dot{E}_d = 0$ (7) where are the $\dot{E}_{in}$,$\dot{E}_S$, $\dot{E}_{out}$, $\dot{E}_l$ and $\dot{E}_d$ inlet, stored, outlet, leakage and destroyed exergy rate, respectively.

The inlet exergy rate includes the inlet exergy rate with fluid flow and the absorbed solar radiation exergy rate. The inlet exergy rate with fluid flow is given by

$$\dot{E}_{in,f} = \dot{m}C_p\left(T_{in} - T_a - T_a \ln\left(\frac{T_{in}}{T_a}\right)\right) + \frac{\dot{m}\Delta P_{in}}{\rho} \quad (8)$$

$$\dot{E}_{in,Q} = \eta_o I_T A_p\left(1 - \frac{T_a}{T_s}\right) \quad (9)$$

Outlet exergy rate is givenby,

$$\dot{E}_{out,f} = -\dot{m}C_p\left(T_{out} - T_a - T_a \ln\left(\frac{T_{out}}{T_a}\right)\right) - \frac{\dot{m}\Delta P_{out}}{\rho} \quad (10)$$

Exergy loss is given by,

$$\dot{E}_l = -U_1 A_p (T_p - T_a)\left(1 - \frac{T_a}{T_p}\right) \quad (11)$$

Exergy destructions are given by,

$$\dot{E}_{d,\Delta T_s} = -\eta_o I_T A_p T_a\left(\frac{1}{T_p} - \frac{1}{T_s}\right) \quad (12)$$

$$\dot{E}_{d,\Delta P} = -\frac{\dot{m}\Delta P}{\rho}\frac{T_a \ln\left(\frac{T_{out}}{T_a}\right)}{(T_{out} - T_{in})} \quad (13)$$

$$\dot{E}_{d,\Delta T_f} = -\dot{m}C_p T_a\left(\ln\left(\frac{T_{out}}{T_{in}}\right) - \frac{(T_{out} - T_{in})}{T_p}\right) \quad (14)$$

The solar collector exergy efficiency defines the increase of fluid flow exergy upon the primary radiation exergy by the radiation source. Substituting Eqs. (8)–(14) into Eq. (7) and considering the exergy efficiency definition, the second law efficiency equation of the solar collector is derived

$$\eta_{ex} = \frac{\dot{m}\left(C_p\left(T_{out} - T_{in} - T_a \ln\left(\frac{T_{out}}{T_{in}}\right)\right) - \frac{\Delta P}{\rho}\right)}{I_T A_p \left(1 - \frac{T_a}{T_s}\right)} \quad (15)$$

$$\eta_{ex} = 1 - \left\{(1 - \eta_o) + \frac{\dot{m}\Delta P}{\rho I_T A_p \left(1 - \frac{T_a}{T_s}\right)} \frac{T_a \ln\left(\frac{T_{out}}{T_a}\right)}{(T_{out} - T_{in})} + \right.$$

$$\eta o Ta1 - TaTs1Tp - 1Ts + U1(Tp - Ta)IT1 - TaTs1 - TaTp + mCpTaITAP \ln ToutTa - Tout - TinTp1 - TaTs \quad (16)$$

2.4 Properties of nanofluids

Various researchers have published the properties of nanoparticles and thermal properties of nanofluids. Table 1 shows the published density, specific heat and thermal conductivity of different nanoparticles. A few mechanism contributing to improvement in thermal properties of nanofluids such as convective heat transfer and thermal conductivity has been described and as listed by Keblinski et al. [14] such as Brownian motion, particle and heat transfer and liquid interface nanolayer in nanoparticles. However, all these special characteristics cannot be achieved unless the nanoparticles are properly dispersed and stable therefore surfactants are used which provide better dispersion and stability of nanofluids.

Table 1: Properties of nanomaterials and base fluid [15]

Material	Specific heat Cp (J/kg K)	Thermal conductivity, K (W/m K)	Density, ρ(kg/m3)
Alumina (Al2O3)	773	40	3960
Copper Oxide (CuO)	551	33	6000
Titanium Oxide(TiO2)	692	8.4	4230
Silicon di Oxide(SiO2)	765	36	3970
Water (H2O) , base fluid	4182	0.60	1000

Density of nanofluid can be calculated by [16]:

$$\rho_{nf} = (1 - \emptyset)\rho_f + \emptyset\rho_p \quad (17)$$

Specific heat of nanofluid is given by,

$$C_{p,nf} = \frac{(1-\emptyset)\rho_f C_{p,f} + \emptyset\rho_p C_{p,p}}{\rho_{nf}} \quad (18)$$

where $C_{p,nf}$ is the heat capacity of nanofluid (J/kg K), $C_{p,p}$ the heat capacity of nanoparticles (J/kg K), $C_{p,f}$ the heat capacity of base fluid (J/kg K), Ø is the volume fraction of nanoparticles in nanofluid (%).

Viscosity of nanofluids is calculated by

$$\mu_{nf} = \mu_f \frac{1}{(1-\emptyset)^{2.5}} \quad (19)$$

Thermal conductivity of nanofluids is calculated by the correlation recommended by Maxwell.

$$k_{nf} = \left[\frac{k_p + 2 \cdot k_f - 2 \cdot \square \cdot (k_f - k_p)}{k_p + 2 \cdot k_f + \square \cdot (k_f - k_p)}\right] \cdot k_f \quad (20)$$

Prandtl number is calculated by

$$Pr_{nf} = \frac{\mu_{nf} C_{p,nf}}{k_{nf}} \quad (21)$$

Reynold number is calculated by

$$Re = \frac{\rho_{nf} Du}{\mu_{nf}} \quad (22)$$

Nusselt number of nanofluids calculation is given by Xuan and Li [17].

For Re < 2300,

$$Nu = 0.4328\,(1 + 11.285\,ø^{0.754}\,Pe^{0.218})\,Re^{0.333}\,Pr^{0.4} \quad (25)$$

For 2300 < Re < 25000,

$$Nu = 0.0059\,(1 + 7.628\,ø^{0.6886}\,Pe^{0.001})\,Re^{0.9238}\,Pr^{0.4} \quad (26)$$

Where , $\emptyset = \frac{V_n}{V_n + V_f} = \frac{\frac{m_n}{\rho_n}}{\frac{m_n}{\rho_n} + \frac{m_f}{\rho_f}}$

Table 2: Environmental and design conditions for the solar collector

Collector parameters	Value
Type	Black paint header-riser flat plate
Glazing	Double glass
Agent fluid in flow ducts	Water
Adhesive resistance, 1/Cb	Negligible
Length and width of collector	L1=1m, L2= Ap/L1 m
Wind speed, Va	25 m/s
Collector tilt,β	200
Fluid inlet and ambient temperature, Tin=Ta	300 K
Apparent sun temperature, Ts	4350 K
Plate thickness,δ	0.002 m
Effective product transmittance–absorptance or optical efficiency, ηo = (τα)	0.84
Emissivity of the absorber plate, δp	0.92
Emissivity of the covers, ἐc	0.88
Glass covers' distance, ,δ1=,δ2	0.04 m
Thickness of the back insulation, , δp	0.08 m
Thickness of the sides' insulation, , δe	0.04 m
Thermal conductivity of the absorber plate, kp	384 W/mK
Thermal conductivity of the insulation, ki	0.05 W/mK
Incident solar energy per unit area of the absorber plate, IT	500W/m2

Tubes' centre to centre distance, W	0.15 m
Inner diameter of pipes, Di	0.04 m

2.5 Simulation procedure

The thermal, geometric and exergetic models presented is transposed into EES computation program. In the program some of the geometric parameters and operating conditions can be variables (Table 2). The problem considers, etc., as constants subject to eqs. (1) to (6) modelled in the thermal, optical and geometric analysis. Constraints are $0.001 \leq m \leq 0.009$ and $1 \leq A_P \leq 10$.

On solving getting A_P=9.18 m^2 and mass flow rate =.0087kg/s.

3. RESULTS AND DISCUSSION

3.1 Effect of varying volume fraction to the properties of working fluids

Density of nanofluids is function of volume fraction of nanoparticles. It will increase by increasing the volume fraction of nanoparticles. Fig. 2 also shows that CuO nanofluids have the highest possible density as compared to the other fluids based on the higher density of CuO nanoparticles.

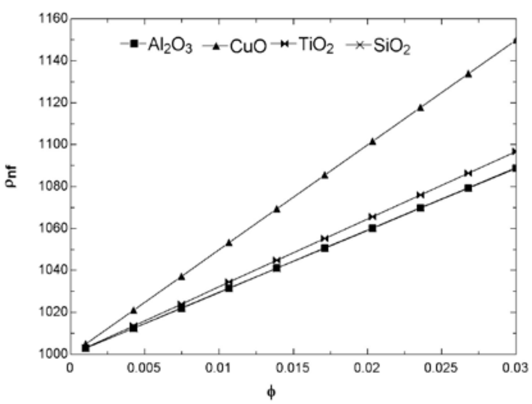

Fig. 2: Variation of density of nanofluids

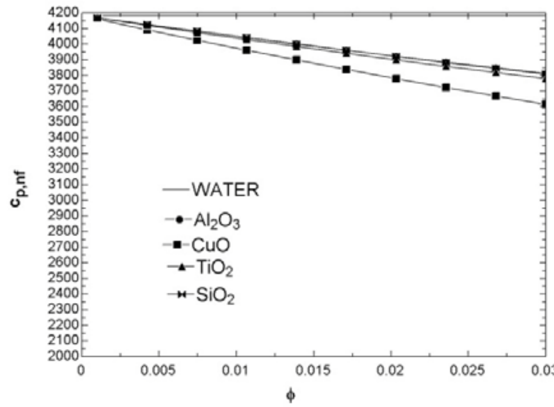

Fig. 3: Variation of heat capacity of nanofluids

Specific heats of nanofluids are inversely proportional to the volume fraction of nanoparticles (Fig. 3). Similar results had also been shown by the other researchers [16]. Specific heat can be explained as the energy required raising the temperature of a unit mass of a substance by one degree. It means that a different amount of heat energy is needed to raise the temperature of similar masses of different substances by one degree. Smaller number of specific heats for nanofluids will leads to smaller amount of energy needed to raise the temperature of nanofluid.

Fig. 4 shows the comparison between the thermal conductivity of nanofluids with different nanoparticle volume fraction (%). In fact, the graph shows that thermal conductivity increases by increasing the nanoparticle volume fraction in basefluid. Al_2O_3 has the highest effect on thermal conductivity improvement of base fluid in comparison with the other investigated nanoparticles.

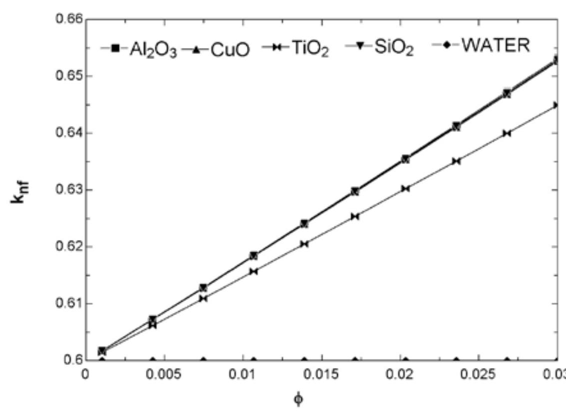

Fig. 4: Nanofluids thermal conductivity variation

3.2 Effect of operating parameters on the solar collector performances

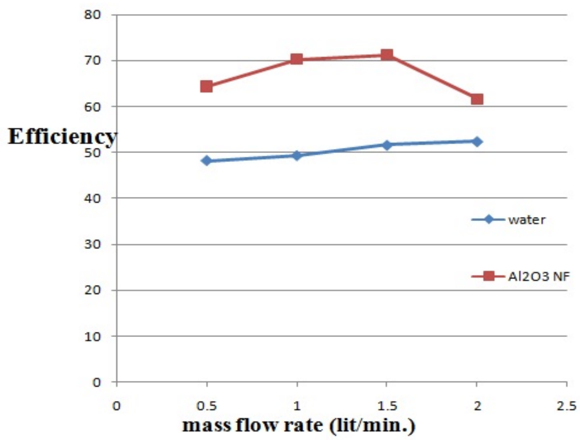

Fig. 5: Variation of thermal efficiency with mass flow rate

Variation of Thermal efficiency with mass flow rate is shown in Fig. 5 for both water and nanofluids. As shown, the performance of flat plate solar thermal collector improves significantly by using nanofluids. After the thermal efficiency of solar collector been determined , potential of collector's area reduction is calculated by substituting efficiency data into Eqs.(27)

$$A_C = \dot{m}C_p(T_{out} - T_{in})/I_T\eta \quad (27)$$

Size reduction calculation is carried out based from variations of efficiency of collectors using different nanofluids (Fig. 6). Efficiency is the dependent on density, specific heat and mass flow rate of different nanofluids calculated with regard to volume fraction of nanoparticles.

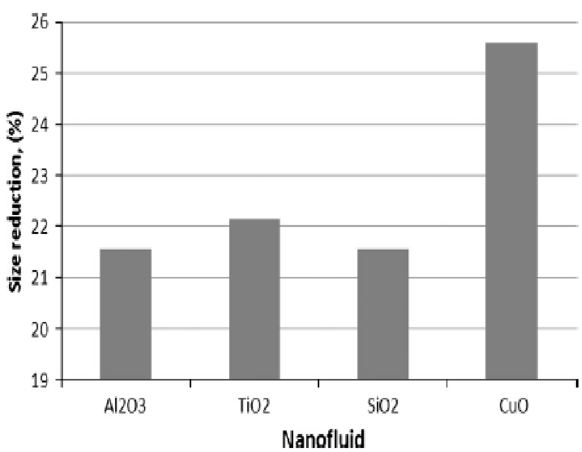

Fig. 6: Percentage of size reduction for solar collector by applying different nanofluids

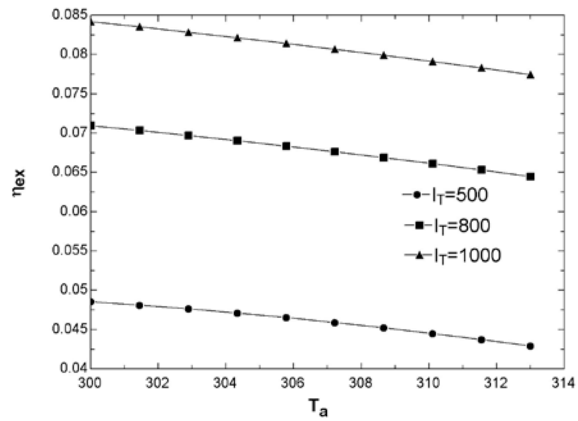

Fig. 7: The variation of exergy efficiency with ambient temperature

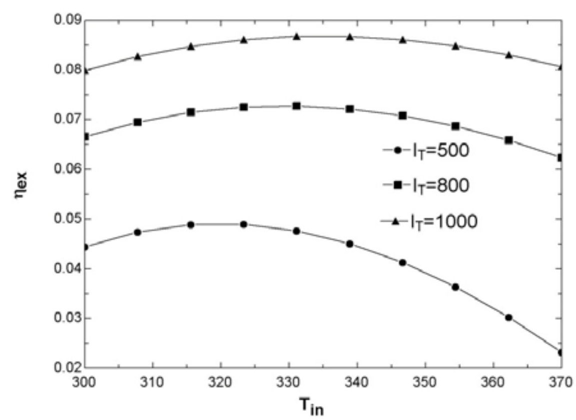

Fig. 8": The variation of exergy efficiency with inlet temperature

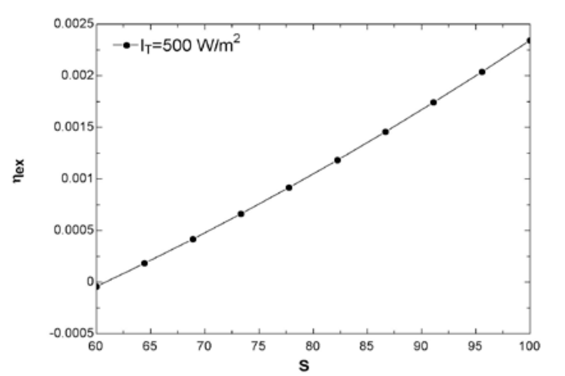

Fig. 9: The variation of exergy efficiency versus optical efficiency.

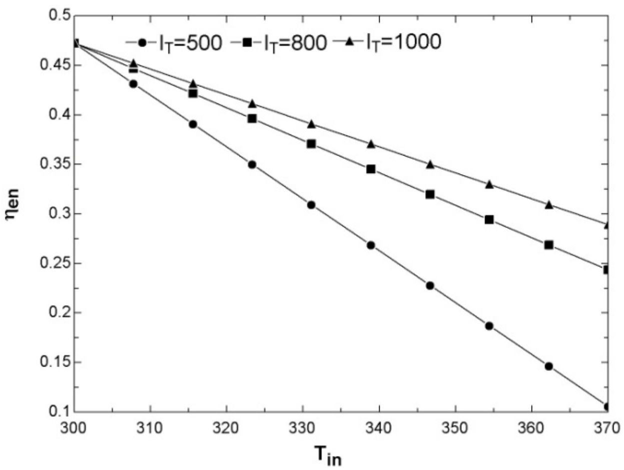

Fig. 10: The variations of the energy efficiency versus inlet temperature

Table 3: Efficiency parameter of the Flat-plate solar collector for water at various flow rates

Mass flow rates (Lit/min)	ηen	ηex
0.5	0.482	0.03829
1.0	0.493	0.03097
1.5	0.516	0.02962
2.0	0.524	0.02875

Fig. s 7-10 show the effects of optical efficiency, ambient temperature and nanofluid inlet temperature on the energy and exergy efficiencies for various global radiation intensities. By increasing the fluid inlet temperature until the value of T_{in}=315 K, the exergy efficiency increases and then decreases quickly and show some optimum value. The thermal efficiency decreases with the increase in fluid inlet temperature. The exegetic efficiency monotonically increases with increase in optical efficiency. The energy and exergy efficiencies of collector with various nanofluid mass flow rate are shown in Table 3. The maximum improvements of about 21% energy efficiency and 2% exergy efficiency have been observed by using nanofluid in the flat plate solar collector (Tables 4).

Table 4: Efficiency ,exergy ,change in efficiency ,change in exergy parameter of the Flat-plate solar collector for Al_2O_3nanofluid mass flow rates

Mass flow rates(Lit/min)	ηen	ηex	Change in ηen	Change in ηex
0.5	0.643	0.05821	15.5	1.992
1.0	0.702	0.05112	20.9	2.015
1.5	0.712	0.0493	19.6	1.968
2.0	0.616	0.03457	9.2	0.582

4. CONCLUSIONS

From results and discussion following conclusions have been made:

a) Addition of trace amounts of aluminium nanoparticles into the basefluid (water) considerably improves its absorption characteristics. This is seen in face of improved thermal and optical efficiencies and higher outlet temperatures.

b) Higher density and lower specific heat of nanoparticles leads to a higher thermal efficiency and CuO nanofluid have the highest value compared to other three nanofluids.

c) Smaller and compact solar collector can be manufactured operated using nanofluids. Hence, it will reduce the weight, energy and cost to manufacture the collector.

d) Solar collector area reduction are achieved for CuO, SiO_2, TiO_2 and Al_2O_3 and it is highest for CuO.

e) By increasing the incident solar energy per unit area of the absorber plate(I_T/A_P), the exergy efficiency increases. It decreases rapidly when the ambient temperature and the wind speed increase.

f) Increasing T_{in} increases the exergy efficiency but there is a maximum point for the nanofluid inlet temperature where the exergy efficiency decreases quickly thereafter.

REFERENCES

[1] Mahian, O., Kianifa, A., Kalogirou, S., Pop, I., and Wongwises, S., “A review of the applications of nanofluids in solar energy”, *International Journal of Heat and Mass Transfer*, 57, 2013, pp. 582-594.

[2] Tyagi, H., Phelen, P., and Prasher, R., “Predicted efficiency of a low-temperature nanofluid based direct absorption solar collector”, *J ournal of Solar Energy Engineering*, 131, 2009, 41004–10.

[3] Nagarajan, P.K., Subramani, J., Suyambazhahan, S., Sathyamurthy, R., “Nanofluids for solar collector applications: A review”, *Energy Procedia*, 61, 2014, pp. 2416-2434.

[4] Taylor, R.A., Phelan, P.E., Otanicar, T.P., Walker, C.A., Nguyen, M., Trimble, S., and Prasher, R., “Applicability of nanofluids in high flux solar collectors”, *Journal of Renewable and Sustainable Energy*, 3, 2011, 023104.

[5] Yousefi, T., Veysi, F., Shojaeizadeh, E., Zi-nadini, S., “An experimental investigation on the effect of Al_2O_3-H_2O nanofluid on the efficiency of flat-plate solar collectors”, *Renewable Energy*, 39, 2012, pp. 293-298.

[6] Yousefi, T., E. Shojaeizadeh, F.Veysi, and S. Zinadini. 2012. “An experimental investigation on the effect of pH variation of MWCNT–H_2O nanofluid on the efficiency of a flat-plate solar collector”, *Solar Energy*, 86, pp. 771–779.

[7] Tiwari, A.K., Ghosh, P., Sarkar, J., “Solar water heating using nanofluids - A comprehensive overview and environmental impact analysis”, *International Journal of Emerging Technology and Advanced Engineering*, 3, 2013, pp. 221-224.

[8] Javadi, F.S., Saidur, R., Kamalisarvestani, M., “Investigating performance improvement of solar collectors by using nanofluids”, *Renewable and Sustainable Energy Reviews*, 28, 2013, pp. 232–245.

[9] Al-Shamani, A.N., Yazdi, M.H., Alghoul, M.A., Abed A.M., Ruslan, M.H., Mat, S, Sopian K., “Nanofluids for improved efficiency in cooling solar collectors – A review”, *Renewable and Sustainable Energy Reviews*, 38, 2014, pp. 348–367.

[10] Hussain, H.A., Jawad, Q., Sultan, K.F., "Experimental analysis on thermal efficiency of evacuated tube solar collector by using nanofluids', *International Journal of Sustainable and Green Energy*, 4, 2015, pp. 19-28.

[11] Kasaeian, A., Eshghi, A.T., Sameti, M., "A review on the applications of nanofluids in solar energy systems", *Renewable and Sustainable Energy Reviews*, 43, 2015, pp. 584–598.

[12] Sarkar, J., Performance of a flat-plate solar thermal collector using supercritical carbon dioxide as heat transfer fluid, *International Journal of Sustainable Energy*, 32, 2013, pp. 531-543.

[13] Sukhatme, S.P., Solar energy. New York: McGraw-Hill; 1993. pp. 83–139.

[14] Keblinski, P., Phillpot, S.R., Choi, S.U.S., Eastman, J.A., Mechanism of heat flow in suspensions of nanosized particles (nanofluids), *International Journal of Heat and Mass Transfer*, 45, 2002, pp. 855–863.

[15] Kamyar, A., Saidur, R., Hasanuzzaman, M., Application of computational fluid dynamics (CFD) for nanofluids. *International Journal of Heat and Mass Transfer*, 55, 2012, pp. 4104–4115.

[16] Zhou, S.Q., Ni, R.. Measurement of the specific heat capacity of water-based Al_2O_3 nanofluid. *Applied Physics Letters*, 92, 2008, pp. 1–3.

[17] Xuan, Y., Li, Q., "Investigation of convective heat transfer and flow features of nanofluids", *Journal of Heat Transfer*, 125, 2003, pp. 151–155.

[18]